Extended Data:

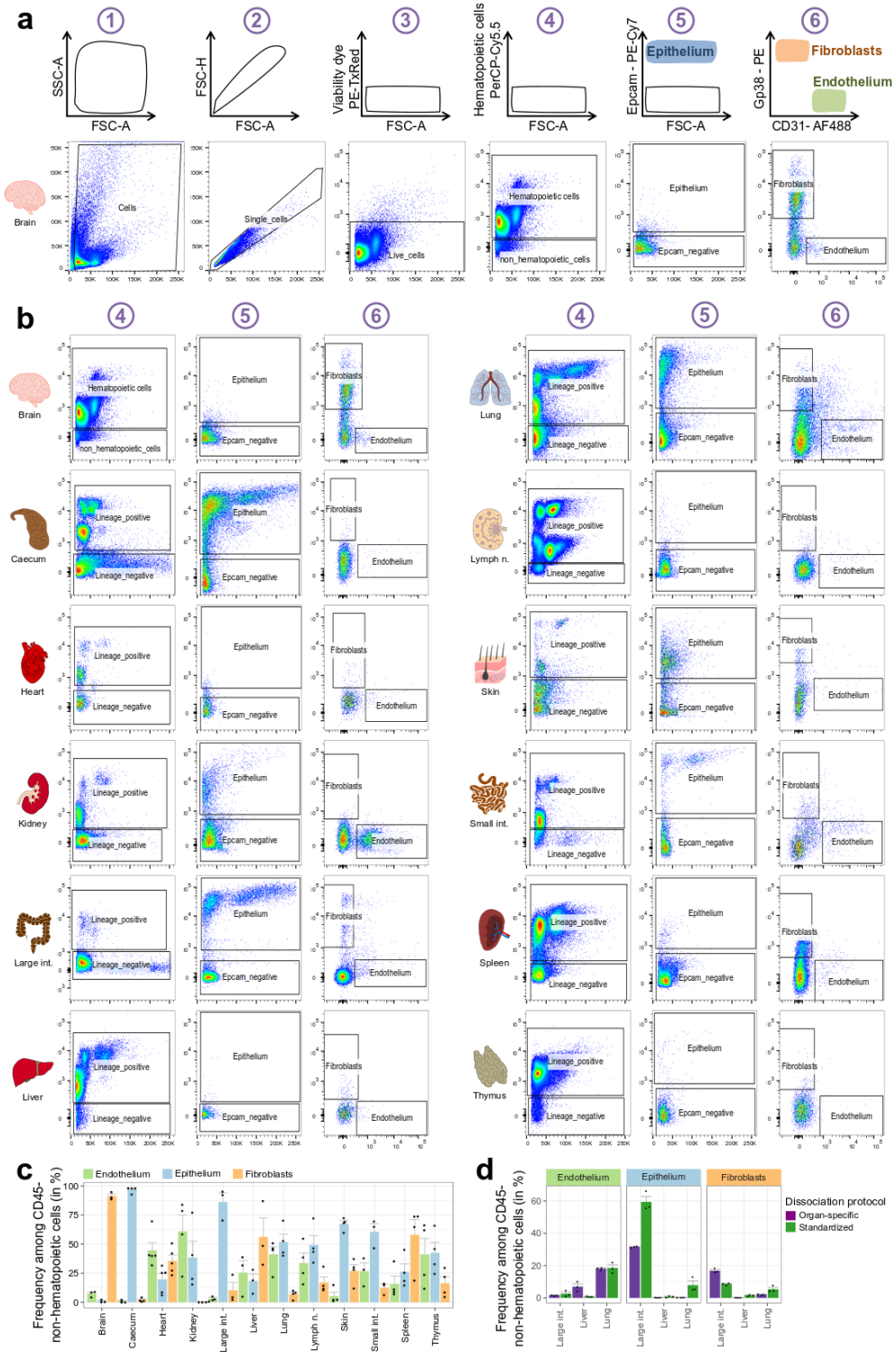

Extended Data Fig. 1. Standardized identification and purification of structural cells across 12 organs. **a**, Cell-type identification and cell sorting scheme (top row) and representative flow cytometry plots (selected from n=4 independent biologically replicates) in one representative organ (brain) under homeostatic conditions (bottom row). **b**, Representative plots (selected from n=4 independent biologically replicates) for gating steps 4 to 6 of the standardized cell-type identification and cell sorting scheme (panel a) across the 12 organs under homeostatic conditions. **c**, Relative frequencies of structural cell types among non-hematopoietic (CD45-) cells across 12 organs, for cell suspensions obtained by standardized organ dissociation. **d**, Relative frequencies of structural cell types among non-hematopoietic (CD45-) cells across three organs, for cell suspensions obtained by either standardized organ dissociation or organ-specific dissociation protocols. Shown are mean and s.e.m. values. Sample size: n = 4 (c) and n = 3 (d) independent biological replicates.

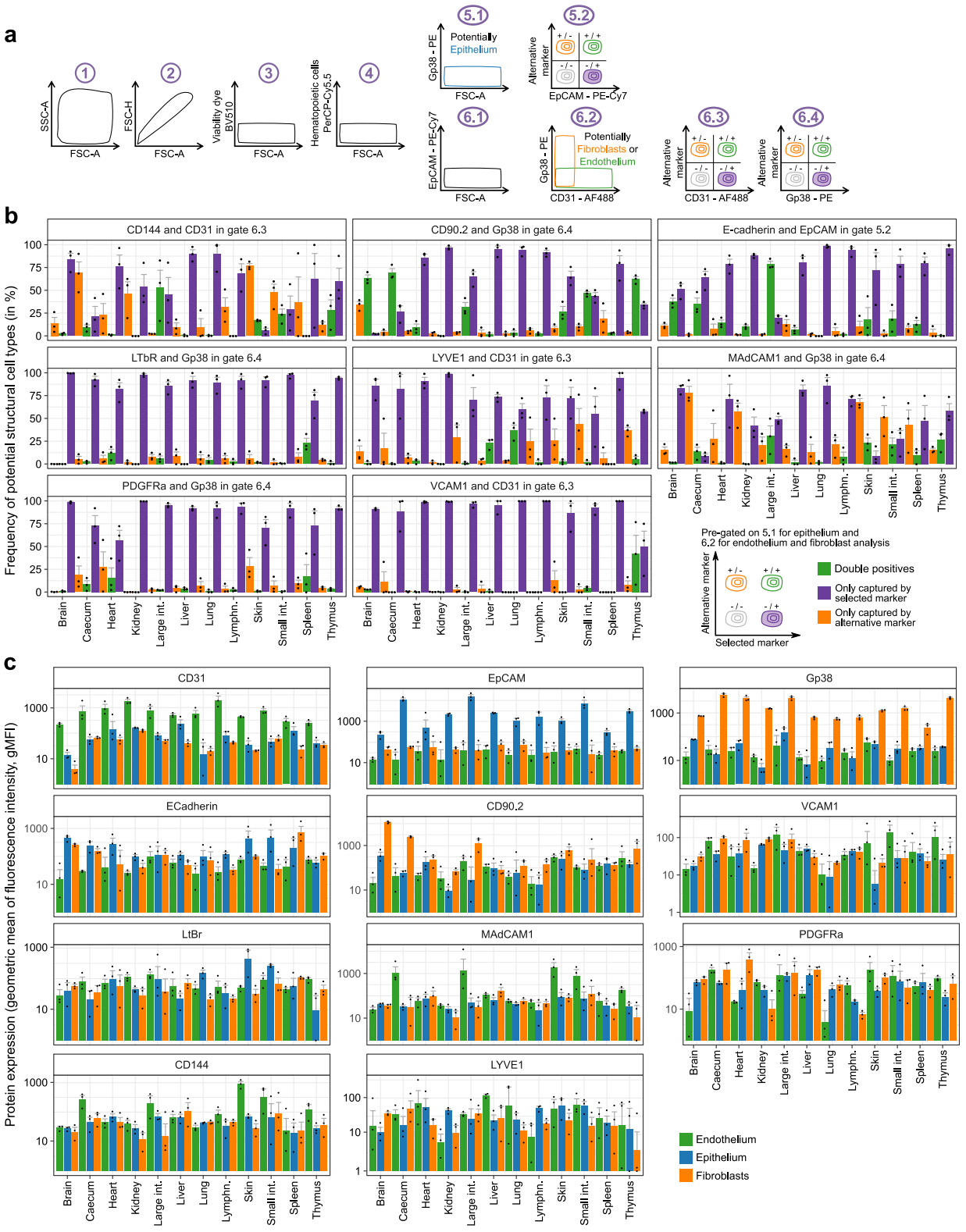

Extended Data Fig. 2. Surface marker profiling of structural cells under homeostatic conditions. **a,** Gating strategy for the flow cytometry-based validation of the structural cell sorting scheme. Identification of structural cells starts with gating for intact cells (1), single cells (2), live cells (3) and non-haematopoietic cells (4). From the resulting non-haematopoietic (CD45$^-$) cell population, potential epithelial cells (5.1) are gated for epithelial cell markers (5.2). Similarly, potential endothelial cells and fibroblasts (6.1, 6.2) are gated for endothelial cell markers (6.3) and fibroblast markers (6.4). **b**, Relative frequencies of potential structural cell types based on gates 5.2, 6.3 and 6.4 (from **a**), comparing the selected markers with alternative markers. **c**, Expression of the selected surface markers of structural cell types (top row) and potential alternative markers for cells gated as in Extended Data Fig. 1a. Shown are mean and s.e.m. values. Sample size (all panels): n = 3 independent biological replicates.

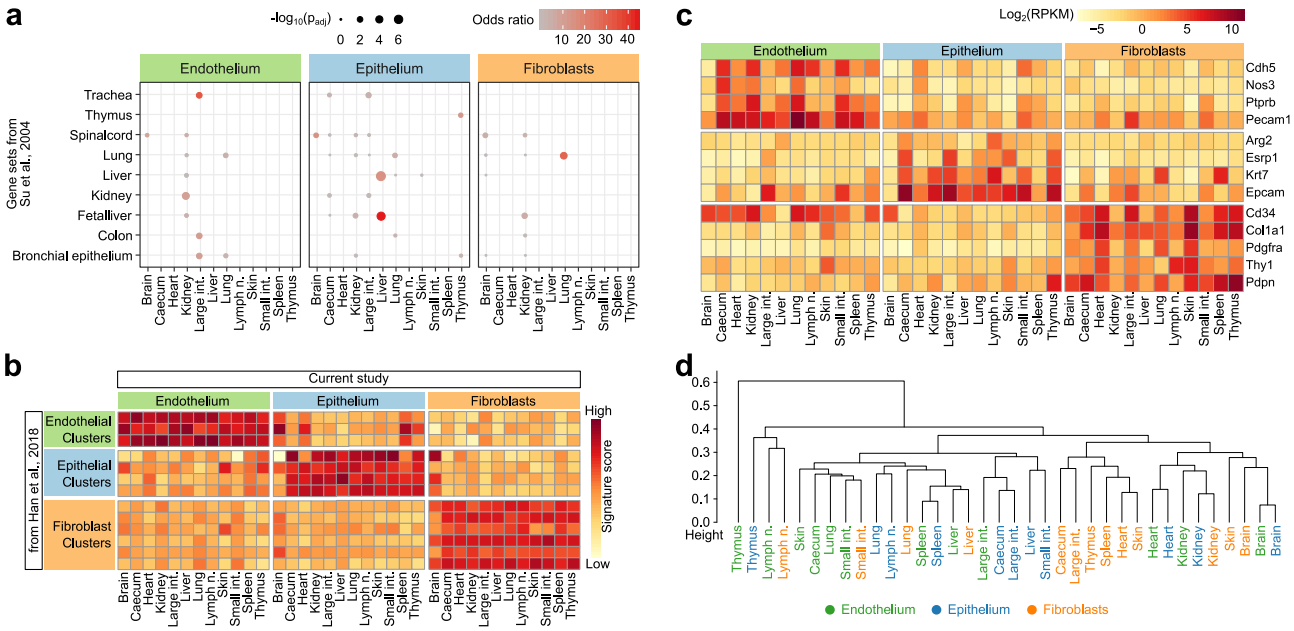

Extended Data Fig. 3. Comparison of the structural cell transcriptomes to published reference data. **a**, Overlap of the identified cell-type-specific and organ-specific marker genes (derived from the RNA-seq experiments in the current study) with tissue-specific gene sets from a microarray-based expression atlas (two-sided Fisher's exact test with multiple-testing correction). **b**, Gene expression across cell types and organs (from the current study) aggregated across marker genes of structural cell clusters in a single-cell RNA-seq atlas of the mouse[19]. **c**, Gene expression across cell types and organs (from the current study) plotted for a manually curated list of commonly used markers of structural cells. **d**, Hierarchical clustering of structural cells across cell types and organs based on the transcriptome profiles from the current study. Sample size (all panels): n = 3 independent biological replicates.

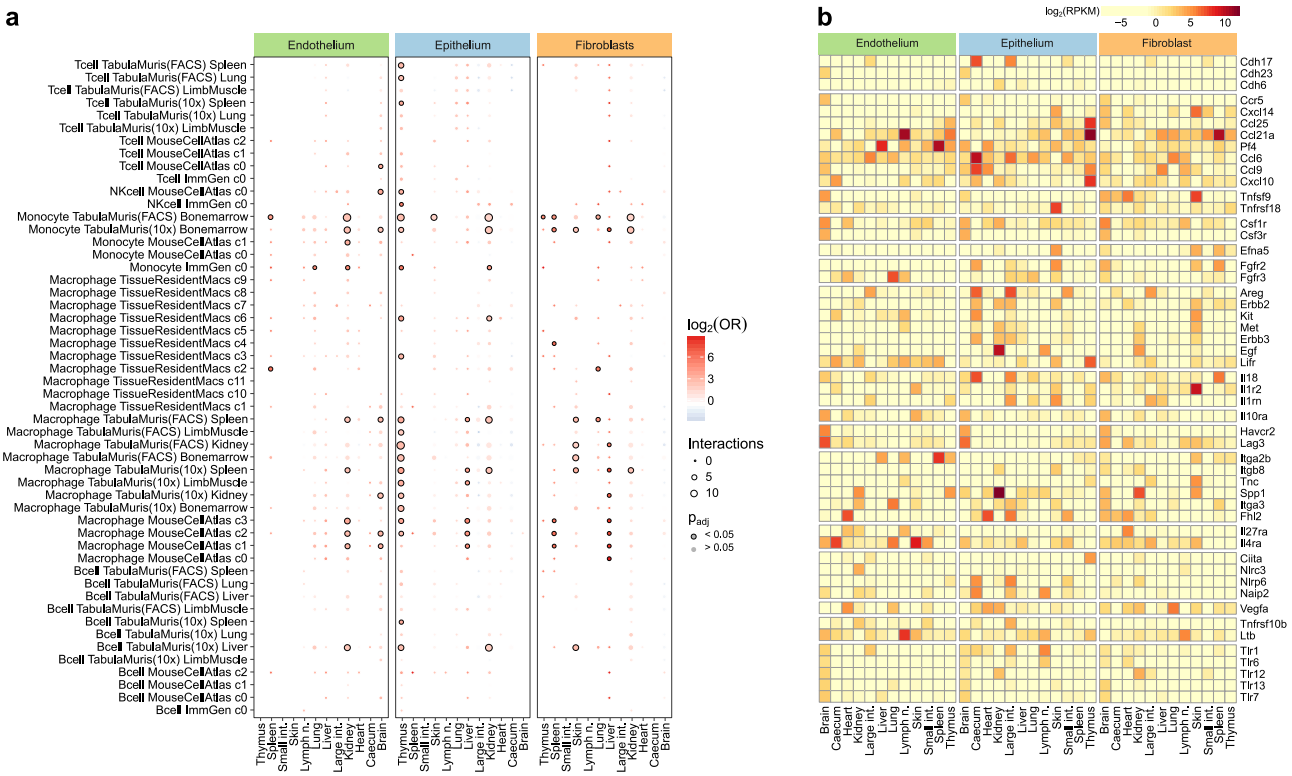

Extended Data Fig. 4. Inference of cell-cell interactions across cell types and organs. **a**, Enrichment analysis for potential cell-cell interactions between structural cells and hematopoietic immune cells, based on gene expression of known receptor-ligand pairs (two-sided Fisher's exact test with multiple-testing correction). For each combination of one structural cell type and one hematopoietic immune cell type, the analysis assesses whether all pairs of marker genes between the two cell types are enriched for annotated receptor-ligand pairs. **b**, Differently expressed genes across cell types and organs, based on a manually curated list of receptors and ligands (Supplementary Table 4). Sample size (all panels): n = 3 independent biological replicates.

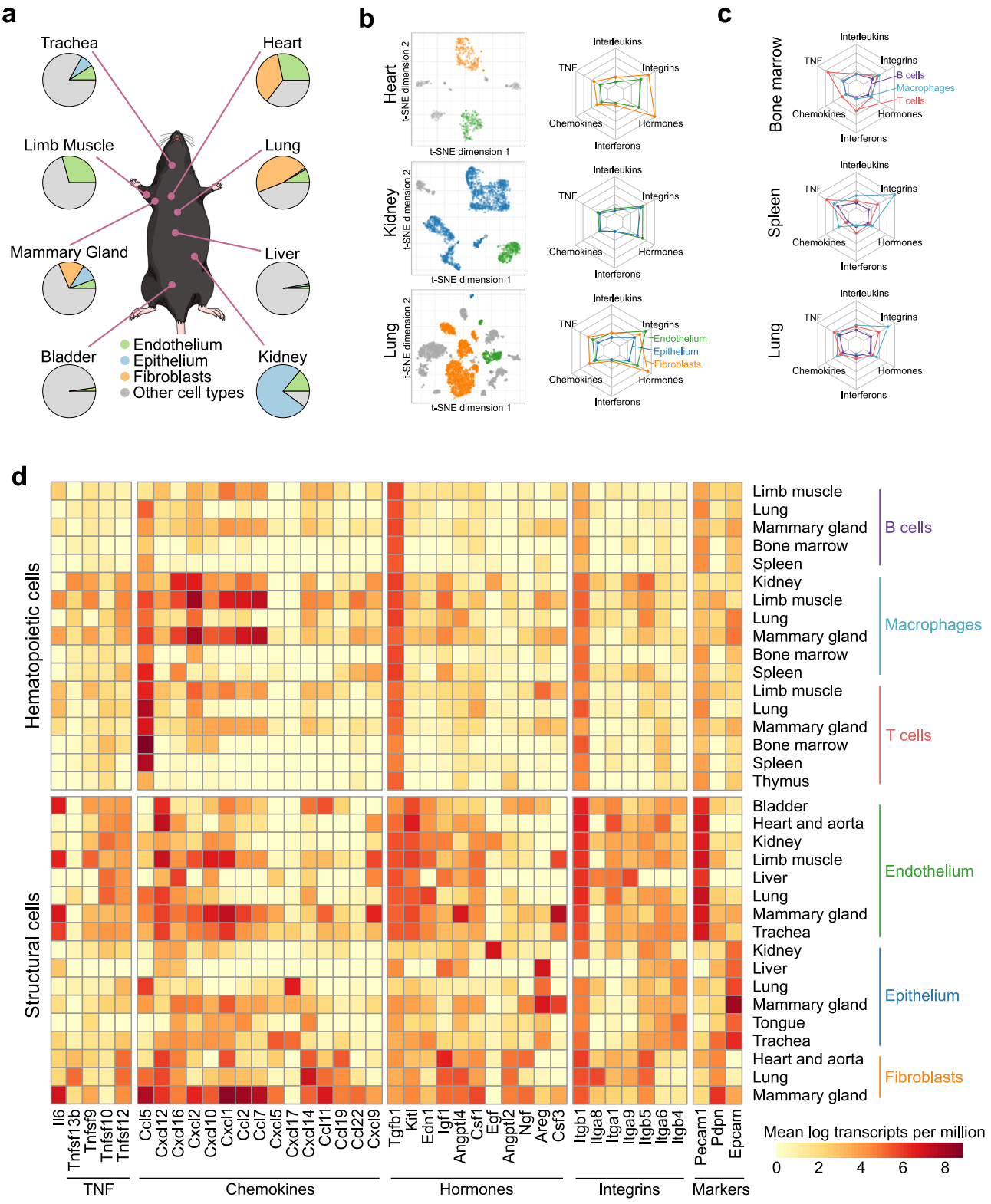

Extended Data Fig. 5. Analysis of immune gene expression among structural cells in an independent dataset. **a**, Relative frequencies of single-cell transcriptomes classified as endothelium, epithelium, and fibroblasts in selected organs according to the Tabula Muris dataset[20]. b, Expression of immune gene signatures in structural cells according to the Tabula Muris dataset, jointly normalized across all plots (for comparability). **c**, Expression of immune gene signatures in hematopoietic immune cells according to the Tabula Muris dataset, normalized in the same way as in panel b. **d**, Expression of selected immune genes in structural cells and in hematopoietic immune cells according to the Tabula Muris dataset. Sample size: n = 7 (all panels) independent biological replicates, comprising 4 male and 3 female mice.

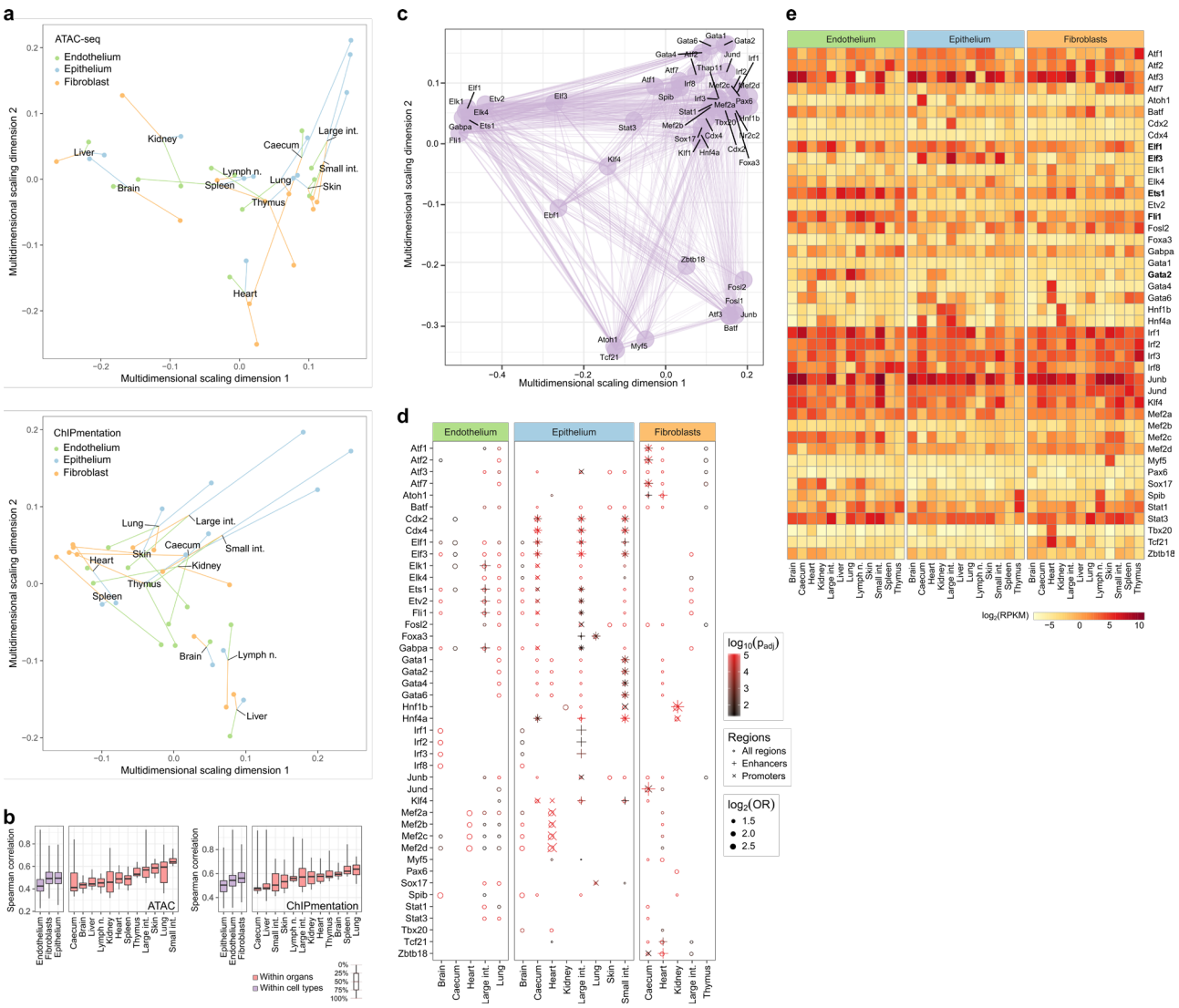

Extended Data Fig. 6. Analysis of transcription regulation in structural cells. **a**, Multidimensional scaling analysis of the similarity of chromatin profiles across cell types, organs, and replicates based on ATAC-seq (top) and H3K4me2 ChIPmentation (bottom). **b**, Correlation of chromatin profiles across cell types and organs for ATAC-seq (left) and H3K4me2 ChIPmentation (right). **c**, Transcriptional regulators of the inferred gene-regulatory network for structural cells, arranged by similarity using multidimensional scaling. **d**, Motif enrichment for transcriptional regulators among differential chromatin peaks, shown separately for each regulator (one-sided hypergeometric test with multiple-testing correction). **e**, Gene expression of the transcriptional regulators across cell types and organs (genes discussed in the text are in bold). Sample size (all panels): n = 2 independent biological replicates.

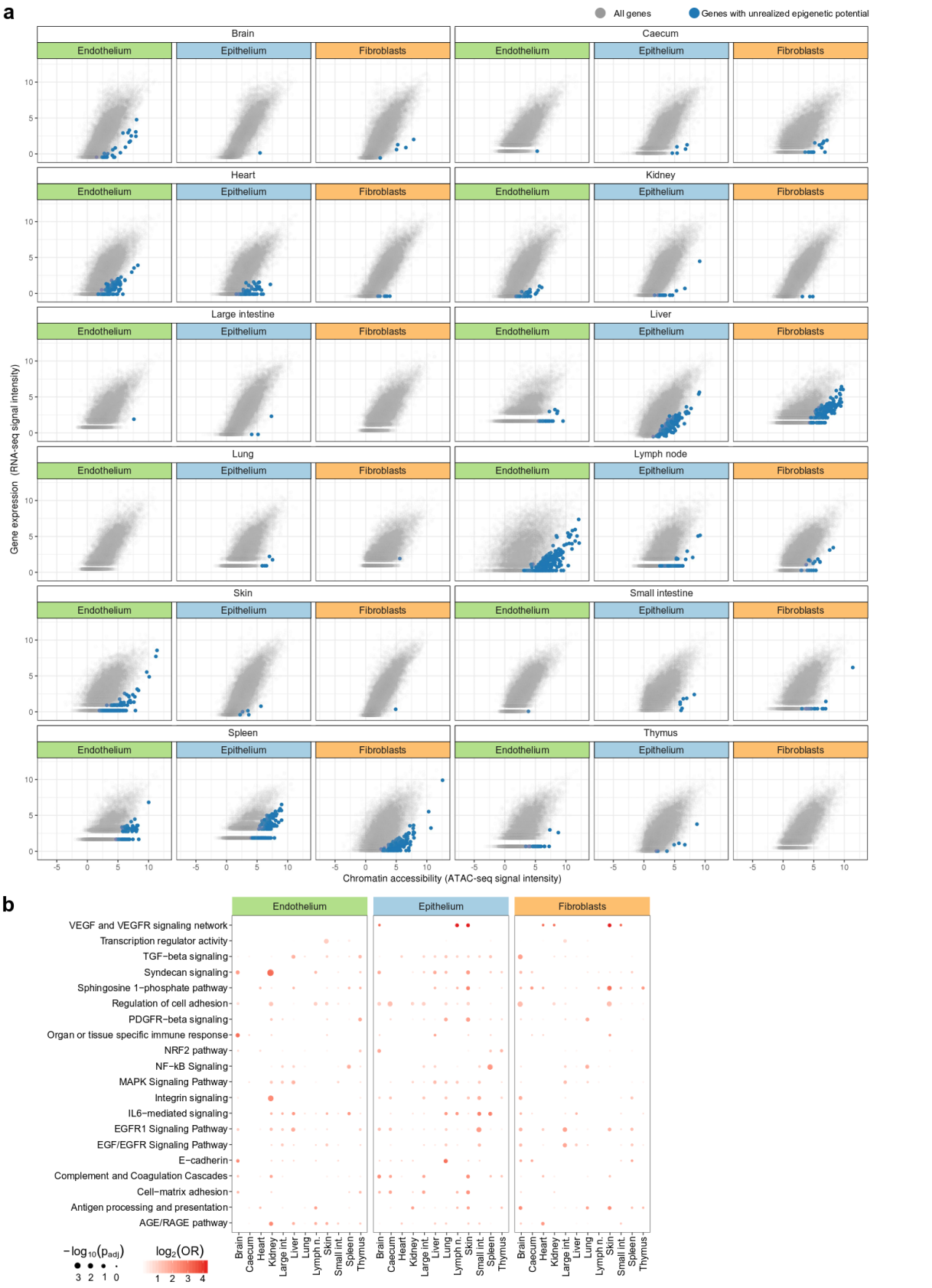

Extended Data Fig. 7. Detection and analysis of genes with unrealized epigenetic potential. **a**, Scatterplot showing the correlation between chromatin accessibility in promoter regions and the corresponding gene expression levels in structural cells across cell types and organs. Genes with significant unrealized epigenetic potential (calculated as the difference between normalized ATAC-seq and RNA-seq signals) are highlighted in blue. **b**, Enrichment of immune-related gene sets among the genes with unrealized epigenetic potential (two-sided Fisher's exact test with multiple-testing correction). Sample size (all panels): n = 2 independent biological replicates.

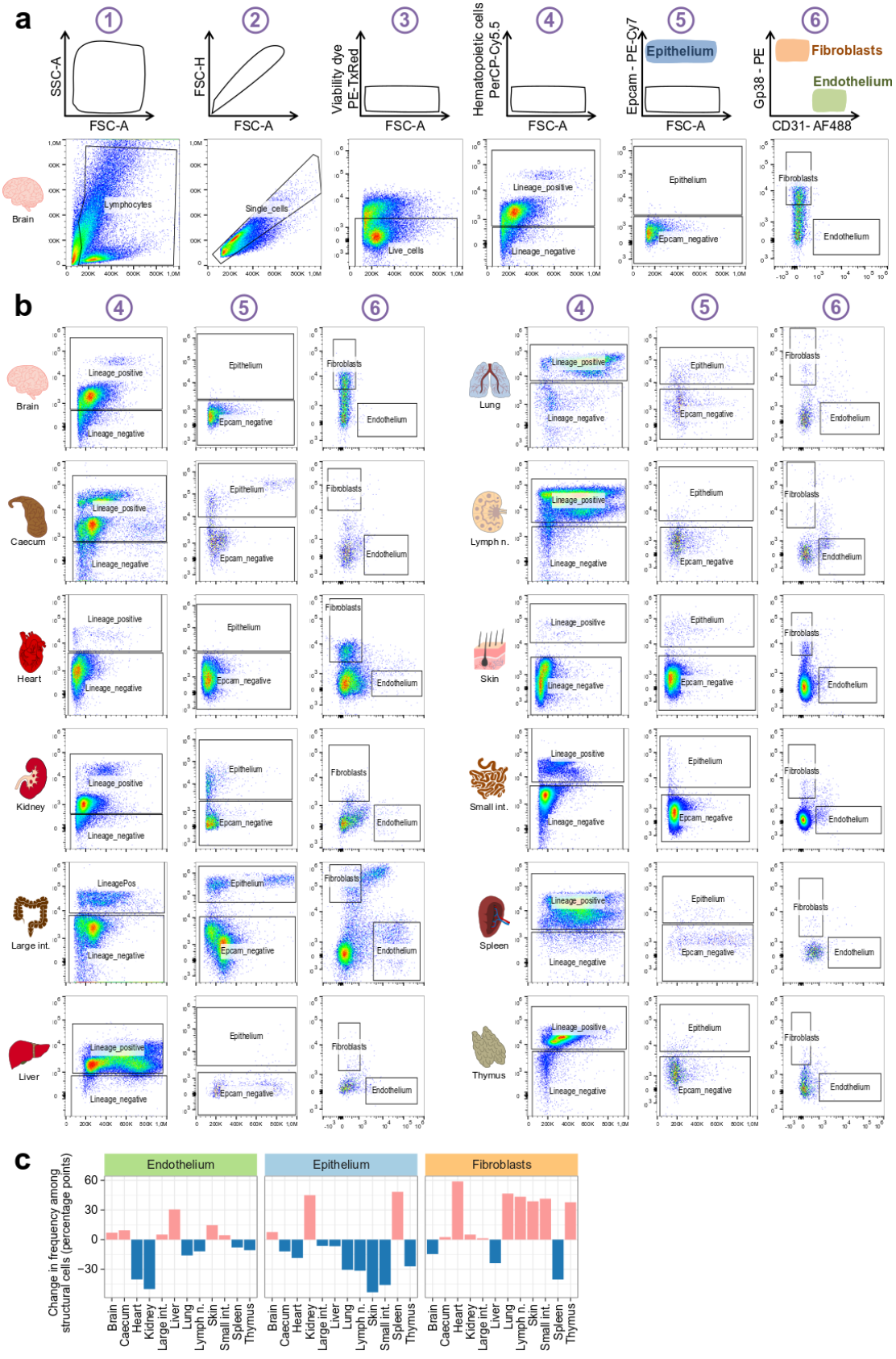

Extended Data Fig. 8. Standardized identification and purification of structural cells after LCMV infection. **a**, Cell-type identification and cell sorting scheme (top row) and representative flow cytometry plots (selected from n=3 independent biologically replicates) in one representative organ (brain) after LCMV infection (bottom row). **b**, Representative plots (selected from n=3 independent biologically replicates) for gating steps 4 to 6 of the standardized cell-type identification and cell sorting scheme (**a**) across the 12 organs upon LCMV infection. **c**, Change in the relative frequenct of structural cells upon LCMV infection. size (all panels): n = 3 independent biological replicates.

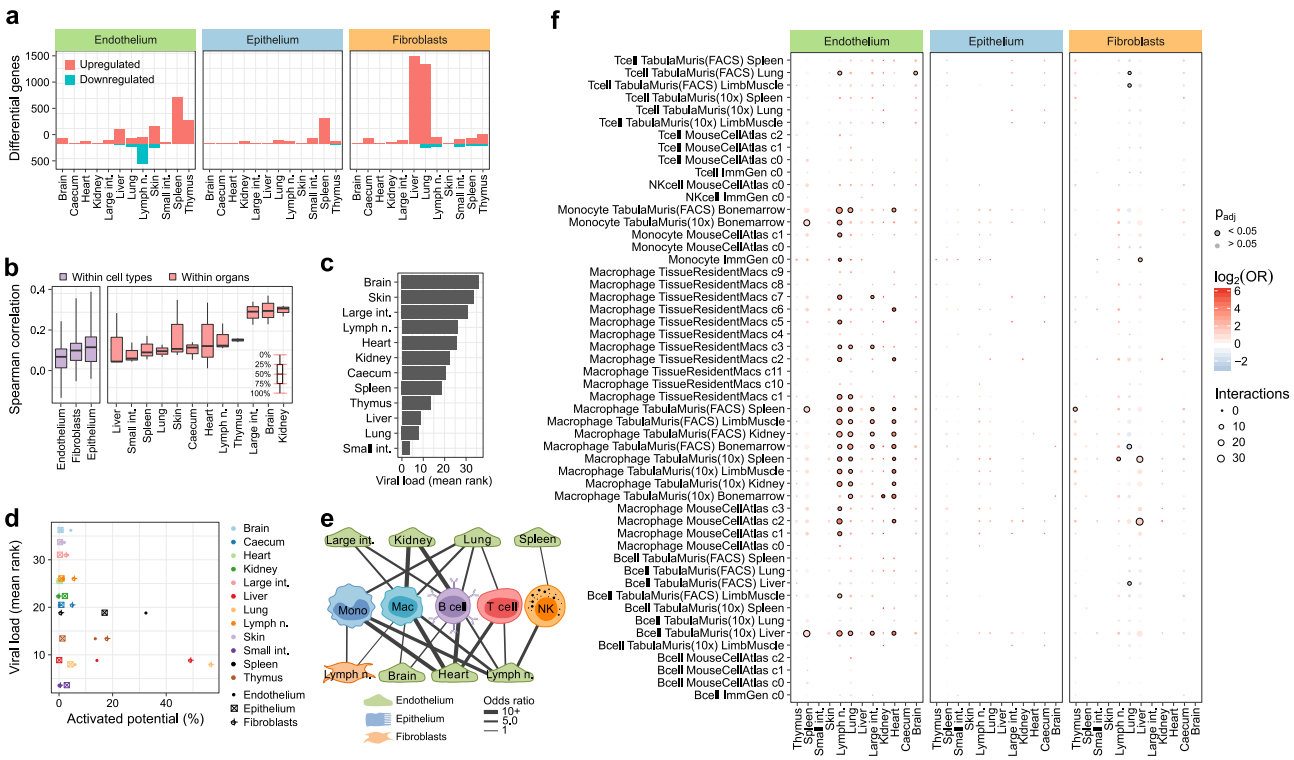

Extended Data Fig. 9. Analysis of differential gene expression in response to LCMV infection. **a**, Number of differentially expressed genes in structural cells upon LCMV infection (this includes not only immune genes but for example also genes associated with the substantial organ-specific tissue damage induced by LCMV infection). **b**, Correlation of the observed changes in gene expression upon LCMV infection across cell types and organs. **c**, Organ-specific viral load at day 8 of LCMV infection, measured by qPCR in whole-tissue samples collected from each organ (without FACS purification of individual cell types). Five reference genes were used for normalization and results were ranked across organs, in order to make the analysis robust toward tissue-specific differences in the expression of these housekeeping genes. However, the experimental results do not support an absolute quantification of viral load in each organ nor do they account for differences in the relative frequencies of cells that are susceptible to LCMV infection in each organ. **d**, Scatterplot illustrating the low correlation between the activated epigenetic potential and the measured viral load across cell types and organs. **e**, Network analysis (**e**) and enrichment analysis (**f**) of potential cell-cell interactions between structural cells and hematopoietic immune cells, inferred from gene expression of known receptor-ligand pairs upon LCMV infection (two-sided Fisher's exact test with multiple-testing correction). For each combination of one structural cell type and one hematopoietic immune cell type, the analysis assesses whether all pairs of marker genes between the two cell types are enriched for annotated receptor-ligand pairs. Sample size: n=3 (all panels).

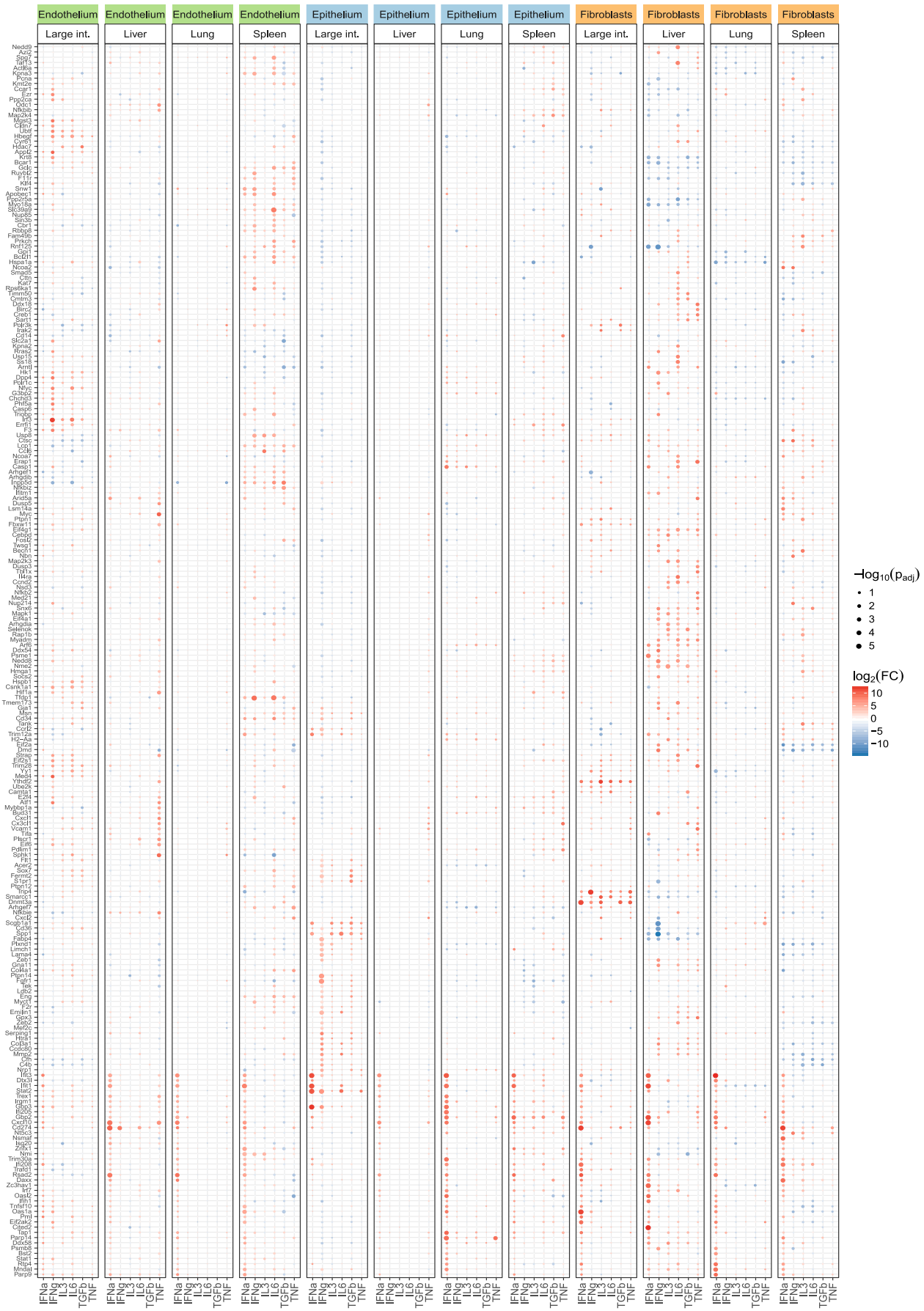

Extended Data Fig. 10. Visualization of differential gene expression in response to *in vivo* cytokine treatments. The heatmap visualizes changes in the expression of genes associated with immune functions, plotted across cell types, organs, and cytokines (two-sided linear model with multiple-testing correction). Sample size: n = 3 independent biological replicates.

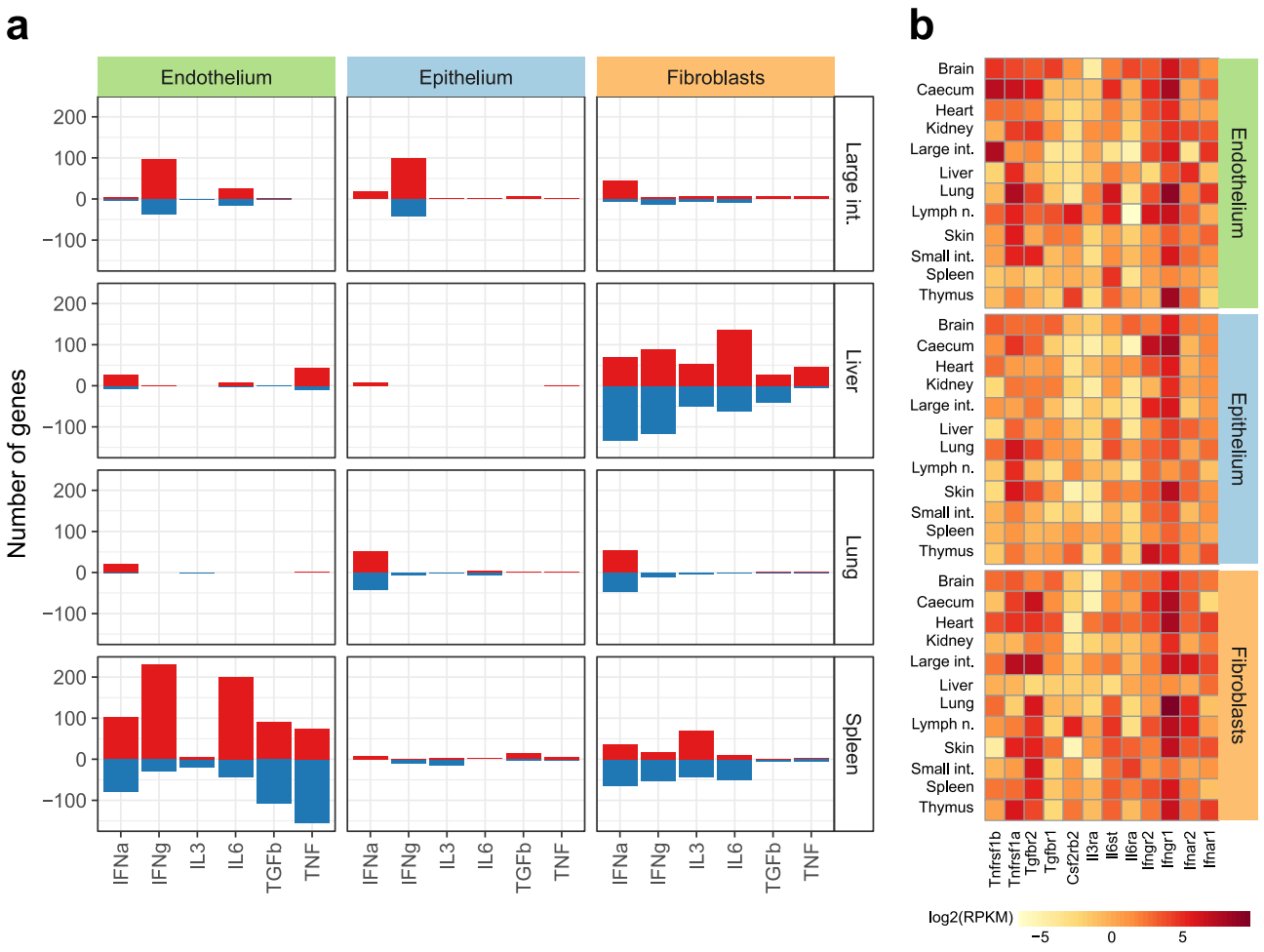

Extended Data Fig. 11. Analysis of differential gene expression in response to *in vivo* cytokine treatments. **a**, Number of differentially expressed genes in response to the individual cytokine treatments. **b**, Gene expression for the known receptors involved in the response to the individual cytokine treatments, plotted across cell types and organs under homeostatic conditions. Sample size (all panels): n = 3 independent biological replicates.

Supplementary Tables:

Supplementary Table 1
Sequencing statistics for RNA-seq, ATAC-seq and H3K4me2 ChIPmentation.

Supplementary Table 2
Cell-type-specific and organ-specific marker genes based on RNA-seq.

Supplementary Table 3
List of receptor-ligand pairs used to construct the cell-cell interaction network under homeostatic conditions.

Supplementary Table 4
Curated list of immune-related receptors and ligands.

Supplementary Table 5
Frequencies of structural cell types per organ in the Tabula Muris dataset.

Supplementary Table 6
Cell-type-specific and organ-specific marker peaks based on ATAC-seq.

Supplementary Table 7
List of genes with unrealized epigenetic potential in structural cells under homeostatic conditions.

Supplementary Table 8
Curated list of immune-related gene sets used for enrichment analysis.

Supplementary Table 9
List of differentially expressed genes upon LCMV infection.

Supplementary Table 10
List of receptor-ligand pairs used to construct the cell-cell interaction network upon LCMV infection.

Supplementary Table 11
List of differentially expressed genes upon cytokine treatment.